

# **Humeral Epiphyseal Shape in the Felidae: The Influence of Phylogeny, Allometry and Locomotion**

Anthony Walmsley,<sup>1</sup> Sarah Elton,<sup>2</sup> Julien Louys,<sup>3-4</sup> Laura C. Bishop,<sup>3</sup> and Carlo Meloro<sup>2</sup>

<sup>1</sup>*Hull York Medical School, The University of York, Heslington York YO10 5DD, UK*

<sup>2</sup>*Hull York Medical School, The University of Hull, Loxley Building Cottingham Road, Hull HU6 7RX, UK*

<sup>3</sup>*Research Centre in Evolutionary Anthropology and Palaeoecology, School of Natural Sciences and Psychology, Liverpool John Moores University, Byrom Street, Liverpool L3 3AF, UK*

<sup>4</sup>*Present address: School of Earth Sciences, The University of Queensland, Brisbane, Australia*

Running Header:

FELID HUMERAL MORPHOLOGY

*Correspondence: Carlo Meloro, Hull York Medical School, The University of Hull, Loxley Building, Cottingham Road, Hull HU6 7RX, UK; T: ++44 (0)1904 321918; F: ++44 (0)1482 466497; [carlo.meloro@hyms.ac.uk](mailto:carlo.meloro@hyms.ac.uk)*

## ABSTRACT

Bone morphology of the cats (Mammalia: Felidae) is influenced by many factors, including locomotor mode, body size, hunting methods, prey size and phylogeny. Here, we investigate the shape of the proximal and distal humeral epiphyses in extant species of the felids, based on two-dimensional landmark configurations. Geometric morphometric techniques were used to describe shape differences in the context of phylogeny, allometry and locomotion. The influence of these factors on epiphyseal shape was assessed using Principal Component Analysis, Linear Discriminant functions and multivariate regression. Phylogenetic Generalised Least Squares was used to examine the association between size or locomotion and humeral epiphyseal shape, after taking a phylogenetic error term into account. Results show marked differences in epiphyseal shape between felid lineages, with a relatively large phylogenetic influence. Additionally, the adaptive influences of size and locomotion are demonstrated, and their influence is independent of phylogeny in most, but not all, cases. Several features of epiphyseal shape are common to the largest terrestrial felids, including a relative reduction in the surface area of the humeral head and increased robusticity of structures that provide attachment for joint-stabilising muscles, including the medial epicondyle and the greater and lesser tubercles. This increased robusticity is a functional response to the increased loading forces placed on the joints due to large body mass.

KEY WORDS: Felidae; humerus; geometric morphometrics; phylogeny; allometry; locomotion

## INTRODUCTION

Accounting for more than ten percent of extant mammalian Carnivora, the Felidae are one of the most well-known families with well over 30 species found on all continents apart from Antarctica and Australia where no endemic species are recorded (Kitchener, 1991; Turner & Antón, 1997; Johnson et al., 2006; MacDonald et al., 2010). All felids are hypercarnivorous, specialised consumers of vertebrates (Kitchener, 1991; Turner & Antón, 1997; Kitchener et al., 2010). This common behaviour has generated relatively conservative cranial and mandibular morphology in the family when compared to other carnivorans (Holliday & Stepan, 2004; Meloro et al., 2008, 2011; Werdelin & Wesley-Hunt, 2010; Meloro, 2011a, b; Meloro & O'Higgins, 2011). In the felid postcranial skeleton, interspecific differentiation has been observed, in part because of adaptations to locomotion and posture (Gonyea, 1976; Van Valkenburgh, 1987; Anyonge, 1996; Andersson & Werdelin, 2003; Meachen-Samuels & Van Valkenburgh, 2009a), but also to adaptations for procuring prey of different sizes (Meachen-Samuels & Van Valkenburgh, 2009a, b, 2010; Lencastre Sicuro, 2011; Lencaster Sicuro & Oliveira, 2011; Meachen-Samuels, 2012) and due to specialisations for different modes of hunting (Christiansen, 2008; Slater & Van Valkenburgh, 2008). Notwithstanding these studies, there is still much to be explored regarding morphological variation in the felid postcranium and the factors, including phylogeny and allometry, that contribute to it.

Felid-like mammals originated in the Oligocene, around 35 million years ago. The earliest stem felid to be identified in the fossil record, *Proailurus*, was

recovered in the Quercy fissures (France) and is dated approximately 28.5 Ma. Molecular data suggest that the modern family Felidae arose within the last 11 million years (Johnson et al., 2006; Werdelin et al., 2010). Based on molecular evidence, the *Panthera* lineage (or clade), comprising the genera *Neofelis* (clouded leopard) and *Panthera* (lion, jaguar, leopard, tiger, snow leopard) is sister to all other extant members of the Felidae (Johnson et al., 2006). This clade originated around six million years ago, with considerable speciation in the genus *Panthera* occurring between around four and two million years ago (Johnson et al., 2006). Three other lineages, the Leopard Cat, Bay Cat and Caracal, diverged at the very end of the Miocene (5-6 Ma), with another, the Puma, originating just less than five million years ago (Johnson et al., 2006). The other lineages (Domestic Cat, Lynx, and Ocelot) diverged in the Pliocene, around three million years ago (Johnson et al., 2006).

Even with a common adaptation to hypercarnivory, the felids demonstrate a large range of body masses, a multitude of behaviours, and marked ecological diversity (Ewer, 1973; Turner & Antón, 1997; MacDonald et al., 2010). Members of the felid family range in size from under three kilograms (e.g. the black footed cat, *Felis nigripes*) to over 300 kilograms (the tiger, *Panthera tigris*). Felids exploit environments as diverse as open desert (e.g. the sand cat, *Felis margarita*), rainforest (e.g. the jaguar, *Panthera onca*), grassland (e.g. the lion, *Panthera leo*) and rocky, mountainous regions (e.g. the bobcat, *Lynx rufus*). Since locomotor mode correlates with the habitat exploited, felids show considerable diversity in locomotion, with some species engaging in

purely terrestrial locomotion and others demonstrating a high degree of arboreality (Ewer, 1973; Kitchener, 1991; Kitchener et al., 2010).

Given the large size range within the felids, allometry is likely to play some role in determining the shape of their postcranial skeletons (Mattern & McLennan, 2000; Diniz-Filho & Nabout, 2009; Meachen-Samuels & Van Valkenburgh, 2009a; Lewis & Lague, 2010). In addition, various studies have implied that phylogeny influences bone morphology within both the carnivoran cranium (Meloro et al., 2008, 2011; Meloro & O'Higgins, 2011) and postcranium (Andersson & Werdelin, 2003; Meloro, 2011a). A small number of studies have examined the relative importance of several factors determining postcranial skeletal form in mammals (Monteiro & Abe, 1999; Young, 2008; Astúa, 2009), but most have focused on single contributory factors, such as locomotor behaviour (Clevedon Brown & Yalden, 1973; Van Valkenburgh, 1987; Carrano, 1999; Schutz & Guralnick, 2007; Polly & MacLeod, 2008; Meloro, 2011c) or allometry (Bertram & Biewener, 1990; Christiansen, 1999, 2002).

In this paper, we examine three factors - phylogeny, size and locomotion – that, alongside other behaviours such as prey capture and foraging, are highly likely to contribute to postcranial bone shape in the felids (Ewer, 1973; Van Valkenburgh, 1987; Turner & Antón, 1997; Meachen-Samuels & Van Valkenburgh, 2009a, 2010; Kitchener et al., 2010; Meachen-Samuels, 2012). Our aim is to provide a detailed description of postcranial bone shape by employing geometric morphometrics in order to quantitatively assess the impact of these factors expressed as percentages of explained variance in shape (cf. Caumul & Polly, 2005). Understanding the factors influencing shape is

important for successfully interpreting the evolutionary history and ecology of this diverse family, and provides a quantitative framework for analysing fossil species.

We focus on the humeral epiphyses partly because the humerus is argued to reflect function, in both felids (Meachen-Samuels & Van Valkenburgh, 2009a, 2010; Lewis & Lague, 2010) and other mammals, including primates and rodents (Elton, 2001, 2002, 2006; Samuels & Van Valkenburgh, 2008). As in primates, the shoulder of many felids is highly mobile and can be used to negotiate complex terrestrial and arboreal environments. Thus, the humerus is often a much better indicator of subtle locomotor differences than hindlimb bones, which tend to provide propulsion (Clevedon Brown & Yalden, 1973). Since the forelimb is load bearing (Day & Jayne, 2007; Doube et al., 2009), the humerus bone itself is also likely to be moulded by allometry, and one would expect the largest felids to exhibit the most robust humeri (Doube et al., 2009; Lewis & Lague, 2010). We thus have three specific research questions:

1. To what extent, if any, phylogeny explains shape variance in the felid humeral epiphyses.

2. To what extent, if any, allometric scaling influences the shape of the epiphyses.

3. To what extent, if any, function (specifically that related to locomotion) influences the shape of the epiphyses.

## **MATERIALS AND METHODS**

### **Specimens and data collection**

Our sample comprised 110 humeri of 32 extant felid species, obtained from collections held at the Natural History Museum London, the National Museum of Scotland and the Royal Museum for Central Africa, with data collected between June 2008 and July 2009 by Meloro. For each species we included the following number of specimens (in parentheses): *Acinonyx jubatus* (5), *Caracal caracal* (2), *Caracal aurata* (2), *Caracal serval* (6), *Felis chaus* (2), *Felis silvestris lybica* (3), *Felis margarita* (2), *Felis nigripes* (2), *Felis silvestris grampia* (9), *Lynx canadensis* (4), *Lynx lynx* (3), *Leopardus pardalis* (4), *Lynx pardinus* (2), *Lynx rufus* (1), *Leopardus wiedii* (1), *Leopardus geoffroy* (2), *Leopardus guigna* (1), *Neofelis nebulosa* (3), *Pardofelis badia* (1), *Pardofelis marmorata* (1), *Pardofelis temminckii* (1), *Prionailurus bengalensis* (4), *Puma concolor* (2), *Puma jagouaroundi* (1), *Panthera leo* (17), *Panthera onca* (3), *Panthera pardus* (12), *Panthera tigris* (4), *Panthera uncia* (4), *Prionailurus planiceps* (1), *Prionailurus rubiginosus* (1), *Prionailurus viverrinus* (4). Details about the studied material are listed for each individual skeletal element in Supplementary online material Table 1.

Two-dimensional images of the humeral epiphyses were captured using a Nikon d40 digital camera with a 200mm lens following a standard protocol. Specimens were placed at a minimum focal distance of one metre from the camera attached to a Manfrotto tripod. A spirit level was used to ensure that the top of the camera remained perpendicular to the specimen being photographed. Eighty two of the 110 images were of the left humerus; the remaining images, of right humeri, were flipped horizontally in tpsDig (version 2.12, Rohlf, 2008) prior to landmarking and analysis. The proximal epiphysis was photographed from

medial and lateral aspects, and the distal epiphysis from anterior and posterior aspects. Data for the distal epiphysis were obtained for all 110 specimens, whereas proximal data were obtained for only 109 specimens.

Landmarks describing the shape of each epiphysis were digitised by Walmsley in tpsDig (Rohlf, 2008) (Fig. 1). Given the potential for increasing statistical error when using Procrustes methods with relatively small sample sizes (Rohlf, 2000, 2003a; Cardini & Elton, 2007), accuracy and precision of landmarking and consequently the amount of digitisation error were assessed. To do this, four specimens, chosen to represent the range of body masses of species in the study, were selected for further landmarking. Two of these, *Leopardus geoffroyi* and *Pardofelis temminckii*, represented species lying within modal frequencies, another belonged to the species with the largest body mass, *Panthera leo*, and the fourth to the species with the smallest body mass, *Prionailurus rubiginosus*. Over a period of three days, each specimen was landmarked according to the scheme illustrated in Fig. 1. Landmarking was repeated a further three times during this period, producing a total of four configurations per specimen. By calculating linear distances between landmarks and assessing how these distances changed after each successive landmarking, it was determined that error due to digitisation was minimal and that landmarks could be repeated with confidence (Supplementary online material Table 2).

## **Data analysis – Geometric morphometrics (GMM)**



The software *morphologika* (O'Higgins & Jones, 2006) was used to conduct Generalised Procrustes Analyses (GPA) and Principal Component Analyses (PCA). GPA superimposes the raw coordinates of each landmark configuration by removing the effects of translation and rotation, and also scales these configurations by calculating a unit centroid size (defined as 'the square root of the sum of squared Euclidean distances from each landmark to the centroid of the landmarks') for each specimen (Bookstein, 1989; Adams et al., 2004; Zelditch et al., 2004). After GPA the landmark configurations provided by each specimen lie within the non-Euclidean, Kendall shape space. Specimens are distributed about the mean landmark configuration and are spread throughout this space according to differences in shape (Zelditch et al., 2004; Chen et al., 2005). To analyse shape differences further, the spread of data within the non-Euclidean space is projected onto a Euclidean, linear tangent space (Rohlf, 1996). Interpretation of the resulting shape data requires PCA. This method of analysis provides orthogonal axes (Principal Components, PCs) that successively describe the major aspects of variance of the sample. With the use of mean coordinates plus eigenvectors, PCA allows shape variance for each PC to be demonstrated graphically (Zelditch et al., 2004; Chen et al., 2005). In the present sample, analyses conducted using tpsSmall version 1.20 (Rohlf, 2003b) indicated there was a very strong correlation ( $r = 0.999$ ) between non-Euclidean and Euclidean tangent space. Thus, the linear tangent space demonstrated by the PC plots reliably describes shape variance amongst specimens.

## Phylogeny

Specimens were grouped according to lineage (Johnson et al., 2006, Supplementary online material Table 1) in order to assess the extent of phylogenetic influence on shape. For each epiphyseal aspect, plots of PC1 vs. PC2 were produced. The shape variance demonstrated by the PC plots was visualised via transformation grids. These transformation grids, formed using thin plate splines, show the relative deformation of structures (Bookstein, 1991), in this case across each PC. The relationship between phylogenetic lineage and shape was investigated by creating dummy variables for each lineage, which were regressed against the multivariate shape data (all PCs). This determined the correlation between phylogeny and shape using a test equivalent to a MANOVA (multivariate analysis of variance), with significance calculated via the Wilks' Lambda test. This test, performed for each aspect of the whole sample (N=109 or 110) in tpsRegr version 1.37 (Rohlf, 2009), also indicates the percentage of shape variance explained by phylogeny.

## Allometry

The influence of allometry on shape variance was investigated via multivariate regression (Monteiro, 1999) performed in *morphologika* (O'Higgins & Jones, 2006). Natural log (NLog) transformed centroid size values were regressed against all PCs collectively, with significance computed using the Wilks' Lambda. Transformation grids were used to illustrate changes in shape from the median sized specimens to the smallest and largest (based on NLog centroid size values).

## Locomotion

Similar methods to those employed in the phylogeny multivariate regression were used to examine the relationship between locomotor mode and shape. Species were assigned to one of three locomotor categories, 'Terrestrial', 'Terrestrial but Climbs' and 'Terrestrial and Arboreal' (Supplementary online material Table 1), based on classifications in Ortolani & Caro (1996). Dummy variables for the three locomotor groups were regressed against shape. Additionally, discriminant function analysis (DFA) was used to explore the changes in shape, as well as size, across locomotor categories. Both shape (PCs) and size (NLog centroid size) variables were used in discriminant analyses, performed for each epiphyseal aspect in PASW version 18 (SPSS Inc., 2009) using a stepwise method (variables are entered into the model if the significance level of their F value is less than 0.05, and they are removed if the significance level is greater than 0.01) to select the variables which best discriminate locomotor categories. Following a recent study (Meloro, 2011a), size has been included alongside shape variables (cf. Schultz & Guralnick, 2007) to increase prediction likelihood of ecological categories. The locomotor categories assigned *a priori* were the same as those used in the regression analyses. Shape variance across each function was visualised by regressing discriminant function scores against shape variables in tpsRegr version 1.37 (Rohlf, 2009), with transformation grids at either extreme of the axes demonstrating deformation from the mean shape. The locomotor groups of the unclassified/unknown specimens were predicted based on data provided by

the discriminant functions. A 'leave-one-out' procedure was conducted as a cross validation.

### **Sensitivity analyses**

In order to validate the efficacy of our discriminant models, to make predictions irrespective of unequal taxonomic sample size (Kovarovic et al., 2011), we performed two kinds of sensitivity analyses. First, we repeated the most accurate DFA after removing from the original sample all the specimens belonging to a particularly abundant taxon. We repeated the DFA by excluding first *Panthera leo* (N = 17, the most abundant 'Terrestrial' felid), then *Felis silvestris grampia* (N = 9, the most abundant 'Terrestrial but Climbs'), and finally *Neofelis nebulosa* (N = 3, representative of 'Terrestrial and Arboreal').

A second sensitivity analysis was conducted to test for the effect of sample size (number of specimens) or body mass (in grams, log transformed) on percentage of correctly classified specimens for the 32 extant species sampled. Non-parametric Spearman correlation was applied to identify positive or negative significant correlations based on the results from all the DFA models.

### **Phylogenetic Generalised Least Squares (PGLS)**

PGLS regressions were performed for each epiphyseal aspect, to assess if differences in shape between specimens as described by locomotion or allometry alone were independent of phylogeny (or specifically whether they were independent of the lineage to which they belong). This method, which can

also be used for multivariate datasets, incorporates phylogeny as an error term within the regression models of shape variables on locomotion (transformed into dummy variables) or size (Martins & Hansen, 1997; Rohlf, 2001, 2006a; Adams, 2008). For these analyses, we computed the mean shape coordinates for each species, performing separate GPAs for each species subsample (cf. Meloro et al., 2008). Size for each species was represented by NLog centroid size averaged from multiple specimens. The phylogenetic covariance matrix was computed based on the topology and time of divergence (from Johnson et al., 2006) and then added as error term in the multivariate regression models in NTSYS 2.21c (Rohlf, 2006b).

## RESULTS

### Phylogeny

MANOVA indicates that shape differs significantly between lineages (Table 1). Phylogeny accounts for the greatest shape variance for the anterior aspect of the distal epiphysis and least for the medial aspect of the proximal epiphysis. For the lateral aspect of the proximal epiphysis, PC1 and PC2 collectively describe 88.09% of the shape variance (PC1, 58.93%; PC2, 29.16%) (Fig. 2A). Even though some overlap between lineages is evident, the Puma lineage tends to cluster at more negative PC1 values, whereas Ocelot, Leopard Cat and Domestic Cat lineages have more positive values. Specimens having extreme negative scores on PC1 have a greater tubercle that projects superiorly above the humeral head, and a humeral head with little posterior projection, whilst specimens with positive scores have a more superiorly and

posteriorly projecting humeral head with a wider articular surface. Lineages overlap more on PC2, which describes the antero-posterior expansion of the greater tubercle associated with reduction of the articulating area of the humerus head (Fig. 2A).

For the medial aspect of the proximal epiphysis, PC1 and PC2 explain 69.07% of the shape variance (PC1, 35.99%; PC2, 33.08%). Overlap occurs between lineages on both axes (Fig. 2B). However, specimens belonging to the *Panthera* and Domestic Cat lineages exhibit negative PC1 and PC2 scores respectively (Fig. 2B). PC1 describes variation in the posterior projection of the humeral head associated with variation in the width of the lesser tubercle. On PC2, specimens with the most negative scores have a more posteriorly projecting humeral head and a greater tubercle with relatively little projection in the superior plane.

For the anterior aspect of the distal epiphysis, PC1 and PC2 collectively describe 72.94% of the shape variance (PC1, 62.69%; PC2, 10.25%). All lineages tend to cluster well along PC1, although Ocelot specimens cluster better on PC2 (Fig. 2C). On PC1, specimens at the positive end of the axis have a more proximally positioned supracondyloid foramen and a relatively smaller combined medio-lateral width of the trochlea and capitulum. On PC2, from negative to positive, there is a relative superior-inferior expansion of the trochlea and capitulum (Fig. 2C).

For the posterior aspect of the distal epiphysis, PC1 and PC2 collectively describe 56.72% of the shape variance (PC1, 36.40%; PC2, 20.32%). Some lineage-based clustering is evident (Fig. 2D), with *Panthera* specimens, for

example, being at the more positive end of PC1, with a relatively larger olecranon fossa area and relatively smaller trochlea/capitulum in the superior-inferior dimension. From negative to positive PC2 scores there is a relative reduction in the medial projection of the medial epicondyle and a decrease in the width of the distal portion of the trochlea and capitulum plus an expansion in olecranon fossa area.

### **Allometry**

In multivariate regression, NLog centroid size was significantly correlated with shape for both aspects of each epiphysis (Table 2). Allometry explains more shape variance in the anterior aspect of the distal epiphysis than in the posterior aspect, and more in the lateral aspect of the proximal epiphysis compared to the medial. Shape changes in relation to changes in NLog centroid size values are illustrated in Fig. 3. On the lateral aspect of the proximal epiphysis, as NLog centroid size increases, there is a decrease in the humeral head surface area and a slight increase in the proximal projection of the greater tubercle (Fig. 3A). Inspection of transformation grids for the medial aspect of the proximal epiphysis (Fig. 3B) indicates that larger specimens have a relatively larger lesser tubercle. On the anterior aspect of the distal humerus (Fig. 3C), larger specimens have a relatively larger combined width of trochlea and capitulum with a shorter and broader medial epicondyle. Differences on the posterior aspect of the distal epiphysis are less marked, although specimens with high NLog centroid size values show an increase in the olecranon fossa area (Fig. 3D).

## Locomotion

MANOVA indicates that shape differs significantly between locomotor categories for both proximal and distal epiphyses although, in general, locomotor differences account for much less shape variance than do either phylogeny or allometry (Table 3). In DFA, two significant functions were extracted for each aspect except the posterior distal epiphysis (Table 4). Table 5 lists the variables selected after the stepwise for the DFA models, with NLog centroid size being included in three of the four models. Reclassification rates using the 'leave one out' method (Table 6) were above chance for each aspect of the epiphyses, with the anterior aspect of the distal epiphysis being the region that best discriminated between different locomotor groups.

The DFA plots show some discrimination between locomotor groups even if overlap occurs among specimens (Fig. 4). Terrestrial specimens tend to occupy positive scores of DF1 in all structures except in the anterior aspect of the distal epiphysis (Fig. 4C). For the proximal epiphysis positive scores of DF1 are associated to short articular surface and a wide lesser tubercle (Figs. 4A, B). 'Terrestrial and Arboreal' specimens tend to occupy positive scores of Function 2 for the lateral aspect of the proximal epiphysis, characterised by less superiorly projecting humeral head (Fig. 4A). However, they overlap extensively with 'Terrestrial but Climbs' specimens and this is reflected in the re-classification rate (Table 6).

For the distal epiphysis, terrestrial specimens have positive scores of DF1 that describe a relatively wide medial epicondyle and a large medio-lateral



width of the trochlea (Fig. 4C). Interestingly, Terrestrial and Arboreal specimens share a wider medial epicondyle with a larger superior-inferior dimension of the trochlea and the supracondyloid foramen on the anterior aspect of the distal epiphysis (Fig. 4C). The posterior aspect of the distal epiphysis does not differentiate locomotor groups on either function (Fig. 4D).

As the medial aspect of the proximal epiphysis and the anterior aspect of the distal epiphysis are the best predictors of locomotor category (Table 6), the functions formed by their shape and size variables are used to predict the locomotor categories for the four specimens of unclassified/unknown locomotion. In the case of the medial aspect of the proximal epiphysis, *Pardofelis badia* and *Pardofelis temminckii* are classified as 'Terrestrial and Arboreal' and both *Felis nigripes* specimens are classified as 'Terrestrial but Climbs'. For the anterior aspect of the distal epiphysis, *Pardofelis badia* and both *Felis nigripes* specimens are classified as 'Terrestrial and Arboreal', whereas *Pardofelis temminckii* is classified as 'Terrestrial but Climbs'.

## Sensitivity Analyses

The percentage of correctly classified specimens differs between species (Table 7). With regard to species with more than one representative specimen, the lion (*Panthera leo*), the snow leopard (*Panthera uncia*) and the cheetah (*Acinonyx jubatus*) appear to be the best classified in the analyses. There is a significant association between body size and number of specimens per species ( $r = 0.62$ ,  $p = 0.0003$ ), but no other factor, including lineage and sample size, affects the reclassification rate.

Separately excluding *Panthera leo*, *Neofelis nebulosa* and *Felis silvestris* specimens (representing the species of largest sample size for each locomotor group) from the discriminant function analyses, does not have a major impact on the reclassification rate of the original DFA models (Table 8). In all cases, the repeated DFA models are statistically significant. There is a small degree of change however, with the exclusion of *Panthera leo* decreasing the reclassification rate for both aspects of proximal epiphyses, whilst removing the *Felis silvestris* sample improved models based on the lateral aspect of proximal epiphysis and the posterior aspect of distal epiphysis. The exclusion of the only three specimens of *Neofelis nebulosa* generally improved reclassification in all the models except for anterior aspect of the distal epiphysis (Table 8).

## PGLS

The PGLS models (Table 9), which incorporate phylogeny as an error term, indicate that allometry has a significant independent influence on humeral epiphyseal shape, except for the anterior aspect of the distal epiphysis. Locomotion has a significant independent influence on the shape of the humeral epiphyses, with the exception of the medial aspect of the proximal epiphysis.

## DISCUSSION

In common with previous research on the felid postcranium (Van Valkenburgh, 1987; Andersson & Werdelin, 2003; Andersson, 2004; Christiansen & Harris, 2005; Doube et al., 2009; Meachen-Samuels & Van Valkenburgh, 2009a), we find clear interspecific variation in long bone

morphology. Phylogeny, allometry and locomotion all influence humeral epiphyseal shape in our sample, with phylogeny and allometry contributing more than locomotion.

Phylogenetic signals in postcranial and cranial shape have been noted among Carnivora as a whole (Radinsky, 1981; Andersson & Werdelin, 2003; Andersson, 2004; Meloro et al., 2008, 2011; Meloro, 2011a, b, c; Meloro & O'Higgins, 2011; Slater & Van Valkenburgh, 2008). MANOVA and PCA in the present study indicate a marked phylogenetic signal in the shape of the humeral epiphyses within the Felidae. For the shape of each aspect of both epiphyses the *Panthera* lineage emerges as one of the most distinctive. This maybe a result of its early divergence from all other cat lineages (Johnson et al., 2006). Such distinctiveness has also been noted in ecomorphological analyses of felid skulls (Werdelin, 1983; Slater & Van Valkenburgh, 2008; Lencastre Sicuro, 2011; Lencastre Sicuro & Oliveira, 2011) and it is apparent when mapping averaged PC1 scores for all the four epiphyseal aspects onto the phylogenetic topology (Fig. 5).

In PCA, members of the *Panthera* lineage tend to form a coherent group separated from most other specimens. This is particularly striking given that the group comprises purely terrestrial, terrestrial with climbing and mixed terrestrial and arboreal species, with a large body mass range (some species being over 150 kg and others under 20kg). However, this diversity is evident in the PC plots and mapping (Figs. 2 and 5). Although the lineage clusters have relatively little overlap with other lineages, wide ranges of scores are still obtained for *Panthera* specimens, for both aspects of the proximal humerus and the

posterior aspect of the distal humerus. This reflects the biological and ecological diversity of modern members of the lineage, which speciated rapidly in the Pliocene (Johnson et al., 2006). Among the other felid lineages, there is considerable overlap on the plots of PC1 versus PC2. Members of the non-*Panthera* lineages tend to be relatively small (17 out of the 26 non-*Panthera* lineage species sampled are under 10kg), and that may account for some overlap, especially since lineages mostly comprising small species tend to be dominated by climbing or arboreal forms, which may create additional convergence. Based on PC1 character mapping, this occurs consistently in the 'Leopard Cat' and 'Domestic Cat' lineages that show a limited variation especially in the lateral aspect of proximal epiphysis and anterior aspect of the distal epiphysis (Fig. 5).

The influence of size on cranial and postcranial morphology has been noted within and between several families of the order Carnivora (Schutz & Guralnick, 2007; Meloro et al., 2008, 2011; Meachen-Samuels & Van Valkenburgh, 2009b; Meloro 2011b). In this study, allometry was a significant influence on humeral epiphyseal shape (accounting for 17–40% of variance), independent of phylogeny for all but the anterior aspect of the distal epiphysis. Allometry explained a reasonably large amount of shape variance for the lateral aspect of the proximal epiphysis. The largest specimens require the greatest amount of stability at the joint to account for increased loading forces. These demonstrate a reduced humeral head surface area, limiting the degree of movement at the shoulder joint, and a more superiorly projecting greater tubercle to reduce rotational movement and to provide a greater surface area

for insertion of the stabilising rotator cuff muscles (Kappelman, 1988; Turner & Antón, 1997).

The shape of the anterior aspect of the distal epiphysis in larger specimens may demonstrate adaptations for stability, including an increased projection of the medial epicondyle for the attachment of muscles that allow pronation-supination as well as flexing digits (i.e. *M. pronator teres*; *M. palmaris longus*; third and fourth parts of *M. flexor profundus digitorum*; *M. flexor carpi radialis*; second head of *M. flexor profundus digitorum*; page 171, Reighard & Jennings, 1901).

The elbow joint is load bearing, and it has been demonstrated that felid limbs respond to increased body size, and therefore increased loading, via allometric shape change (Doubé et al., 2009), so larger species and specimens are more robust. In felids the influence of allometry has been suggested to be much stronger at the epiphyses than at the shaft, due to tension from muscle and ligament attachments and due to shear and torsion from joint loading (Doubé et al., 2009). This allometric pattern is unique to felids, as other carnivoran families (with species exhibiting body masses of less than 300 Kg), such as canids, respond to an increase in body size by limb straightening (Day & Jayne, 2007; Meachen-Samuels & Van Valkenburgh, 2009a).

Interestingly, PGLS shows that size influence is dependent on phylogeny in the anterior aspect of distal epiphysis, suggesting that there is a very strong phylogenetic signal in this region of the bone. The significant independent contribution of locomotion in influencing the anterior distal humerus morphology suggests that there has also been strong selective pressure on this region that is not simply explained by size or conserved morphology. The assertion of

strong selective pressure for the anterior distal epiphysis is reinforced by the reasonably high classification accuracy in discriminant analysis across all locomotor groups (in general, better than the proximal epiphysis or posterior distal aspect for all locomotor categories).

DFA and PGLS indicate that locomotion influences humeral epiphyseal shape, further confirming the association between locomotion and mammalian postcranial shape noted in previous studies (Van Valkenburgh, 1987; Kappelman, 1988; Gebo & Rose, 1993; Plummer & Bishop, 1994; Elton, 2001, 2002; Schutz & Guralnick, 2007; Meachen-Samuels & Van Valkenburgh, 2009b; Meloro 2011a). This notwithstanding, locomotion explained the least amount of humeral epiphyseal shape variance (between 5 and 16%) in our sample. For the medial aspect of the proximal epiphysis, for which locomotion explained the least variance (5%), PGLS indicated that this influence was dependent on phylogeny.

The mean reclassification rate for the whole DFA was 65%, relatively modest compared to studies of other mammals (Kappelman, 1988; Plummer & Bishop, 1994; Bishop, 1999; Elton, 2001), but similar to the rate observed in an earlier study (Meachen-Samuels & Van Valkenburgh, 2009a) of felid forelimb shape that used a different locomotor categorisation system that divided the sample into terrestrial, arboreal and scansorial specimens. Based on data from Ortolani & Caro (1996), the majority of cats are at least partially terrestrial, which may have assisted their extensive dispersal and cosmopolitan range (sensu Hughes et al., 2008). This widespread terrestriality across species

inevitably results in morphological similarity, either because of shared ancestry or convergence, which in turn is reflected in the discriminant analysis.

The DFA classification accuracy rate for the anterior aspect of the distal epiphysis was surprisingly high in the 'Terrestrial but Climbs' category, given the range of species and body masses included and in marked contrast to the modest classification rates of the other humeral aspects for this category. The landmark set for the anterior aspect of the distal humerus captures two important components of the elbow joint: the trochlea, which articulates with the ulna and the capitulum which articulates with the radial head, as well as the medial epicondyle, the origin for mm. flexor carpi radialis, mm. flexor carpi ulnaris, mm. flexor digitorum superficialis (all flexors of the manus) and the manual pronator mm. pronator teres (Kardong & Zalisko, 2002). It is possible that the good separation between 'Terrestrial but Climbs' and other felid specimens reflects differences in manual flexion and pronation in climbing cats. Discrimination was poor for the posterior aspect of the distal epiphysis, a result consistent with the multivariate regression. Given the results for the anterior aspect of the distal humerus, this result may seem anomalous, as the anterior and posterior aspects are part of the same structure. However, the dominant feature of the posterior distal humerus, the olecranon fossa, has been shown in previous studies, albeit in primates, to be highly morphologically variable (Elton, 2001).

For the proximal humerus, as well as the posterior distal epiphysis, large scatters around centroids were evident, with extensive overlap between categories. In our study, there was reasonably high general classification

accuracy in the 'Terrestrial' sample. This reflects, in part, adaptations for terrestriality (including a humeral head with a relatively decreased surface area, and an increased lesser tubercle width and greater tubercle projection for insertion of the rotator cuff muscles) which stabilise the limb and constrain movement mainly to the parasagittal plane, important when chasing prey in open environments (Kappelman, 1988; Gebo & Rose, 1993; Turner & Antón, 1997).

Additionally, our sensitivity analyses demonstrate that DFA models were always accurate irrespective of sample size and species selection.

Classification rate varies across species but this variation has no pattern and is not systematically influenced by any ecological or phylogenetic factor. On the other hand, the exclusion of particular taxa from our sample confirms DFA model stability, where accuracy appears to be unchanged or even increased in some cases. This allows us to interpret with confidence the classification of unknown specimens. The classification of *Pardofelis badia* and *Pardofelis temminckii* is consistent with an arboreal lifestyle. This is likely to reflect the strong phylogenetic component observed in all humeral epiphyses, as these species appear to be classified within the same group as their sister species *Pardofelis marmorata* (Johnson et al., 2006). The same applies for *Felis nigripes*, a species that one would expect to be classified as a terrestrial species (cf. Meachen-Samuels & Van Valkenburgh, 2009), but is in fact classified as either 'Terrestrial but Climbs' or 'Terrestrial and Arboreal'. It is likely that this species retained ancestral adaptations for climbing in humeral



morphology that are not needed for its current habitat preference (short  
grassland of Southern Africa, (MacDonald et al., 2010).

In summary, we have found that whilst the shape of humeral epiphyses  
is strongly informative of Felidae evolutionary history, size and locomotion exert  
an adaptive influence on their interspecific shape variation. Our study provides  
a solid baseline to extend two dimensional geometric morphometric analyses to  
other long bone epiphyses, as well as other mammals.

## ACKNOWLEDGEMENTS

We would like to thank museum curators and staff at British Museum of  
Natural History (NHM, London), the Royal Museum of Scotland (RMS,  
Edinburgh) and the Royal Museum for Central Africa (RMCA, Tervuren) for  
kindly providing access and support to the study of felid skeletal specimens. In  
particular, we are grateful to: P. Jenkins, L. Tomsett, R. Portela-Miguez, A.  
Salvador, and D. Hills (NHM); A. Kitchener and J. Herman (RMS); E. Gilissen  
and W. Wendelen (RMCA). The data collection from the Royal Museum for  
Central Africa was undertaken thanks to a SYNTHESYS grant to C. Meloro for  
the project 'Ecomorphology of extant African carnivores' (BE-TAF 4901). Our  
research was generously supported by the Leverhulme Trust project "Taxon-  
Free Palaeontological Methods for Reconstructing Environmental Change"  
(F/00 754/C). We thank the Editor, M. Starck, and two anonymous reviewers for  
useful suggestions that improved the quality of this manuscript.

## LITERATURE CITED

- 598 Adams DC, Rohlf FJ, Slice DE. 2004. Geometric morphometrics: ten years of  
599 progress following the 'revolution'. *Ital J Zool* 71:5–16.
- 600 Adams DC. 2008. Phylogenetic meta-analysis. *Evolution* 62:567–572.
- 601 Andersson KI, Werdelin L. 2003. The evolution of cursorial carnivores in the  
602 Tertiary: implications of elbow-joint morphology. *Proc Roy Soc Lond B (Suppl)*  
603 270:S163–S165.
- 604 Andersson KI. 2004. Elbow-joint morphology as a guide to forearm and foraging  
605 behaviour in mammalian carnivores. *Zool J Linn Soc* 142:91–104.
- 606 Anyonge W. 1996. Locomotor behaviour in Plio-Pleistocene sabre-tooth cats: a  
607 biomechanical analysis. *J Zool* 238:395–413.
- 608 Astúa D. 2009. Evolution of scapula size and shape in didelphid marsupials  
609 (*Didelphimorphia: Didelphidae*). *Evolution* 63:2438–2456.
- 610 Bertram JEA, Biewener AA. 1990. Differential scaling of the long bones in the  
611 terrestrial Carnivora and other mammals. *J Morphol* 204:157–169.
- 612 Bishop LC. 1999. Suid paleoecology and habitat preference at African Pliocene  
613 and Pleistocene hominid localities. In: Bromage TG & Schrenk F, editors.  
614 *African Biogeography, Climate Change and Early Hominid Evolution*. New York:  
615 Oxford University Press. p 216–225.
- 616 Bookstein FL. 1989. Size and shape: a comment on semantics. *Syst Zool*  
617 38:173–180.
- 618 Bookstein FL. 1991. *Morphometric tools for landmark data. Geometry and*  
619 *Biology*. Cambridge: Cambridge University Press.
- 620 Cardini A, Elton S. 2007. Sample size and sampling error in geometric  
621 morphometric studies of size and shape. *Zoomorphology* 126:121–134.

- 622 Carrano MT. 1999. What, if anything, is a cursor? Categories vs. continua for  
 623 determining locomotor habit in mammals and dinosaurs. *J Zool* 247:29–42.
- 624 Caumul R, Polly PD. 2005. Phylogenetic and environmental components of  
 625 morphological variation: skull, mandible, and molar shape in marmots  
 626 (*Marmota*, Rodentia). *Evolution* 57:2460–2472.
- 627 Chen X, Milne N, O' Higgins P. 2005. Morphological variation of the  
 628 thoracolumbar vertebrae in Macropodidae and its functional relevance. *J*  
 629 *Morphol* 266:167–181.
- 630 Christiansen P. 1999. Scaling of the limb long bones to bodymass in terrestrial  
 631 mammals. *J Morphol* 239:167–190.
- 632 Christiansen P. 2002. Mass allometry of the appendicular skeleton in terrestrial  
 633 mammals. *J Morphol* 251(2):195–209.
- 634 Christiansen P, Harris M. 2005. Body size of *Smilodon* (Mammalia: Felidae). *J*  
 635 *Morphol* 266:369–384.
- 636 Christiansen P. 2008. Evolution of skull and mandible shape in cats (Carnivora:  
 637 Felidae). *PLoS ONE* 3:e2807.
- 638 Clevedon Brown J, Yalden DW. 1973 The description of mammals-2 Limbs and  
 639 locomotion of terrestrial mammals. *Mammal Rev* 3:107–134.
- 640 Day LM, Jayne BC. 2007. Interspecific scaling of the morphology and posture of  
 641 the limbs during the locomotion of cats (Felidae). *J Exp Biol* 210:642–654.
- 642 Diniz-Filho JAF, Nabout JC. 2009. Modeling body size evolution in Felidae  
 643 under alternative phylogenetic hypotheses. *Genet Mol Biol* 32:170–176.

- 644 Doube M, Wiktorowicz-Conroy A, Christiansen P, Hutchinson JR, Shefelbine S.  
 645 2009. Three-dimensional geometric analysis of felid limb bone allometry. PLoS  
 646 ONE 4:e4742.
- 647 Elton S. 2001. Locomotor and habitat classification of cercopithecoid postcranial  
 648 material from Sterkfontein Member 4, Bolt's Farm and Swartkrans Members 1  
 649 and 2, South Africa. *Palaeontologia africana* 37:115–126.
- 650 Elton S. 2002. A reappraisal of the locomotion and habitat preference of  
 651 *Theropithecus oswaldi*. *Folia Primatol* 73:252–280.
- 652 Elton S. 2006. 40 years on and still going strong: the use of the hominin-  
 653 cercopithecoid comparison in human evolution. *J Roy Anthropol Inst* 12:19–38.
- 654 Ewer RF. 1973. *The carnivores*. New York: Cornell University Press.
- 655 Gebo DL, Rose KD. 1993. Skeletal morphology and locomotor adaptation in  
 656 *Prolimnocyon atavus*. *J Vertebr Paleont* 13:125–144.
- 657 Gonyea WJ. 1976. Behavioural implications of saber-toothed felid morphology.  
 658 *Paleobiology* 2:332–342.
- 659 Holliday JA, Steppan SJ. 2004. Evolution of hypercarnivory: the effect of  
 660 specialization on morphological and taxonomic diversity. *Paleobiology* 30:108–  
 661 128.
- 662 Hughes JK, Elton S, & O'Regan HJ. 2008. *Theropithecus* and 'Out of Africa'  
 663 dispersals in the Plio-Pleistocene. *J Hum Evol* 54:43–77.
- 664 Johnson WE, Eizirik E, Pecon-Slattery J, Murphy WJ, Antunes A, Teeling E,  
 665 O'Brien SJ. 2006. The late Miocene radiation of modern Felidae: a genetic  
 666 assessment. *Science* 311:73–77.

- 667 Kappelman J. 1988. Morphology and locomotor adaptations of the bovid femur  
668 in relation to habitat. *J Morphol* 198:19–130.
- 669 Kardong KV, Zalisko EJ. 2002. *Comparative Vertebrate Anatomy: A Laboratory*  
670 *Dissection Guide*. Boston: McGraw-Hill.
- 671 Kitchener A. 1991. *The Natural History of the Wild Cats*. New York: Comstock  
672 Publishing Associates.
- 673 Kitchener AC, Van Valkenburgh B, Yamaguchi N. 2010. Felid form and function.  
674 In: MacDonald DW, Loveridge AJ, editors. *Biology and Conservation of Wild*  
675 *Felids*. Oxford: Oxford University Press. p 83–106.
- 676 Kovarovic K, Aiello LC, Cardini A, Lockwood CA. 2011. Discriminant Function  
677 Analysis in archaeology: are classification rates too good to be true? *J Archaeol*  
678 *Sci* 38:3006–3018.
- 679 Lencastre Sicuro F. 2011. Evolutionary trends on extant cat skull morphology  
680 (Carnivora: Felidae): a three-dimensional geometrical approach. *Biol J Linn Soc*  
681 103:176–190.
- 682 Lencastre Sicuro F, Oliveira FB. 2011. Skull morphology and functionality of  
683 extant Felidae (Mammalia: Carnivora): a phylogenetic and evolutionary  
684 perspective. *Zool J Linn Soc* 161:414–462.
- 685 Lewis ME, Lague MR. 2010. Interpreting sabretooth cat (Carnivora; Felidae;  
686 Machairodontinae) postcranial morphology in light of scaling patterns. In:  
687 Goswami A, Friscia AR, editors. *Carnivoran Evolution. New views on*  
688 *phylogeny, form and function*. Cambridge: Cambridge University Press. p 411–  
689 465.

- 690 MacDonald DW, Loveridge AJ, Nowell K. 2010. *Dramatis personae*: an  
691 introduction to the wild felids. In: MacDonald DW, Loveridge AJ, editors. Biology  
692 and Conservation of Wild Felids. Oxford: Oxford University Press Oxford. p 3–  
693 58.
- 694 Maddison DR, Maddison WP. 2000. MacClade version 4: Analysis of phylogeny  
695 and character evolution. Sinauer Associates, Sunderland Massachusetts.
- 696 Martins EP, Hansen TF. 1997. Phylogenies and the comparative method: a  
697 general approach to incorporating phylogenetic information into the analysis of  
698 interspecific data. Am Nat 149:646–667.
- 699 Mattern MY, McLennan DA. 2000. Phylogeny and speciation of felids. Cladistics  
700 16:232–253.
- 701 Meachen-Samuels J, Van Valkenburgh B. 2009a. Forelimb indicators of prey-  
702 size preference in the Felidae. J Morphol 270:729–744.
- 703 Meachen-Samuels J, Van Valkenburgh B. 2009b. Craniodental indicators of  
704 prey size preference in the Felidae. Biol J Linn Soc 96:784–799.
- 705 Meachen-Samuels J, Van Valkenburgh B. 2010. Radiographs reveal  
706 exceptional forelimb strength in the sabertooth cat, *Smilodon fatalis*. PLoS ONE  
707 5:e11412.
- 708 Meachen-Samuels J. 2012. Morphological convergence of the prey-killing  
709 arsenal of sabertooth predators. Paleobiology 38:1–14.
- 710 Meloro C, Raia P, Piras P, Barbera C, O'Higgins P. 2008. The shape of the  
711 mandibular corpus in large fissiped carnivores: allometry, function and  
712 phylogeny. Zool J Linn Soc 154:832–845.

- 713 Meloro C. 2011a. Feeding habits of Plio-Pleistocene large carnivores as  
714 revealed by their mandibular geometry. *J Vertebr Paleont* 31:428–446.
- 715 Meloro C. 2011b. Morphological disparity in Plio-Pleistocene large carnivore  
716 guilds from Italian peninsula. *Acta Palaeontol Pol* 56:33–44.
- 717 Meloro C. 2011c. Locomotor adaptations in Plio-Pleistocene large carnivores  
718 from the Italian peninsula: Palaeoecological implications. *Current Zoology*  
719 57:269–283.
- 720 Meloro C, O' Higgins P. 2011. Ecological adaptations of mandibular form in  
721 fissiped Carnivora. *J Mamm Evol* 18:185–200.
- 722 Meloro C, Raia P, Carotenuto F, Cobb S. 2011. Phylogenetic signal, function  
723 and integration in the subunits of the carnivoran mandible. *Evol Biol* 38:465–  
724 475.
- 725 Monteiro LR. 1999. Multivariate regression models and geometric  
726 morphometrics: the search for causal factors in the analysis of shape. *Syst Biol*  
727 48:192–199.
- 728 Monteiro LR, Abe AS. 1999. Functional and historical determinants of shape in  
729 the scapula of Xenarthran mammals: evolution of a complex morphological  
730 structure. *J Morphol* 241:251–263.
- 731 O' Higgins P, Jones N. 2006. *Morphologika 2.5*, York: Function morphology &  
732 evolution research group, Hull York Medical School.
- 733 Ortolani A, Caro TM. 1996. The adaptive significance of color patterns in  
734 carnivores: phylogenetic tests of classic hypotheses. In: Gittleman JL, editor.  
735 *Carnivore Behaviour, Ecology, and Evolution*, Vol. 2. New York: Cornell  
736 University Press. p 132–188.

- 737 Plummer TW, Bishop LC. 1994. Hominid Paleoecology at Olduvai Gorge,  
738 Tanzania as indicated by antelope remains. *J Hum Evol* 27:47–75.
- 739 Polly PD, Macleod N. 2008. Locomotion in fossil carnivora: an application of  
740 eigensurface analysis for morphometric comparison of 3D surfaces.  
741 *Palaeontologia Electronica* 11.2.8A.
- 742 Radinsky LB. 1981. Evolution of skull shape in carnivores, 1: representative of  
743 modern carnivores. *Biol J Linn Soc* 15:369–388.
- 744 Reighard JE, Jennings, HS. 1901. *Anatomy of the Cat*. New York: H. Holt.
- 745 Rohlf FJ. 1996. Morphometric spaces, shape components and the effect of  
746 linear transformations. In: Marcus LF, Corti M, Loy A, et al., editors. *Advances*  
747 *in morphometrics*. New York: Plenum Press. p 131–129.
- 748 Rohlf FJ. 2000. On the use of shape spaces to compare morphometric  
749 methods. *Hystrix Ital J Mamm* 11:8–24.
- 750 Rohlf FJ. 2001. Comparative methods for the analysis of continuous variables:  
751 geometric interpretations. *Evolution* 55:2143–2160.
- 752 Rohlf FJ. 2003a. Bias and error in estimates of mean shape in morphometrics. *J*  
753 *Hum Evol* 44:665–683.
- 754 Rohlf FJ. 2003b. tpsSmall1.20. Stony Brook, NY: Department of Ecology and  
755 Evolution, State University of New York.
- 756 Rohlf FJ. 2006a. A comment on phylogenetic correction. *Evolution* 60:1509–  
757 1515.
- 758 Rohlf FJ. 2006b. NTSYSpc 2.21c. New York: Exeter Software.
- 759 Rohlf FJ. 2008. tpsDig2.12. Stony Brook, NY: Department of Ecology and  
760 Evolution, State University of New York.



- 761 Rohlf FJ. 2009. tpsRegr1.37. Stony Brook, NY: Department of Ecology and  
762 Evolution, State University of New York.
- 763 Slater GJ, Van Valkenburgh B. 2008. Long in the tooth: evolution of sabertooth  
764 cat cranial shape. *Paleobiology* 34:403–419.
- 765 Samuels JX, Van Valkenburgh B. 2008. Skeletal indicators of locomotor  
766 adaptations in living and extinct rodents. *J Morphol* 269:1387–1411.
- 767 Schutz H, Guralnick RP. 2007. Postcranial element shape and function:  
768 assessing locomotor mode in extant and extinct mustelids carnivorans. *Zool J*  
769 *Linn Soc* 150: 895–914.
- 770 SPSS Inc. 2009. PASW Statistics 18.0. Chicago: IBM company headquarters.
- 771 Turner A, Antón M. 1997. *The Big Cats and their fossil relatives*. New York:  
772 Columbia University Press.
- 773 Van Valkenburgh B. 1987. Skeletal Indicators of Locomotor Behaviour in Living  
774 and Extinct Carnivores. *J Vertebr Paleont* 7:162–182.
- 775 Werdelin L. 1983. Morphological patterns in the skulls of cats. *Biol J Linn Soc*  
776 19:375–391.
- 777 Werdelin L, Wesley-Hunt G. 2010. The biogeography of carnivore  
778 ecomorphology. In: Goswami A, Friscia A, editors. *Carnivoran Evolution: New*  
779 *Views on Phylogeny, Form and Function*. New York: Cambridge University  
780 Press. p 225–245.
- 781 Werdelin L, Yamaguchi N, Johnson WE, O'Brien SJ. 2010. Phylogeny and  
782 evolution of cats (Felidae). In: MacDonald DW, Loveridge AJ, editors. *Biology*  
783 *and Conservation of Wild Felids*. Oxford: Oxford University Press. p 59–82.

Young, N.M. 2008. A Comparison of the Ontogeny of Shape Variation in the Anthropoid Scapula: Functional and Phylogenetic Signal. *American Journal of Physical Anthropology*. 136:247–264.

Zelditch ML, Swiderski DL, Sheets HD, Fink WL. 2004. *Geometric morphometrics for biologists. A primer*. Amsterdam: Elsevier.

## FIGURE CAPTIONS

**Fig. 1** The location of landmarks digitised for each epiphyseal aspect.

Landmarks are placed to represent anatomical loci of functional significance.

Scale bars represent 10 millimetres. Dotted lines demonstrate how angular and

linear measurements were used to obtain landmarks geometrically. A = Lateral

aspect of the proximal epiphysis, B = Medial aspect of the proximal epiphysis, C

= Anterior aspect of the distal epiphysis, D = Posterior aspect of the distal

epiphysis. Anatomical position of each landmark as follows: (A1, B1) Most distal

point on the humeral head; (A2) proximal junction between humeral head and

greater tubercle; (A3\*) lies on the anterior surface of the humerus and is

perpendicular to the line connecting landmarks A1 & A2, at the level of

landmark A2; (A4, B8) proximal tip of the greater tubercle; (A5\*) furthest

projection of the humeral head, at a distance halfway between landmarks A1 &

A2; (B2) most anterior and most distal point on the lesser tubercle; (B3) most

anterior and most proximal point on the lesser tubercle; (B4\*) lies on the

anterior surface of the humerus and is perpendicular to the line connecting

landmarks B1 & B3, at the level of landmark B3; (B5) most posterior and most

distal point on the lesser tubercle; (B6) most posterior and most proximal point on the lesser tubercle; (B7\*) furthest projection of the humeral head at a distance halfway between landmarks B1 & B6; (C1, D2) distal tip of the trochlea; (C2, D3) distal junction between the trochlea and capitulum; (C3, D4) most distal and most lateral point on the capitulum; (C4, D1) most proximal and most lateral point on the capitulum; (C5) proximal tip of the trochlea; (C6) proximal tip of the supracondyloid foramen; (C7, D7) most medial point on the medial epicondyle; (D5) proximal tip of the olecranon fossa; (D6) most lateral point on the lateral epicondyle; (D8\*) lies on the medial surface of the olecranon fossa and is perpendicular to the line connecting landmark D1 & D4, at the level of landmark D1. \*Landmark obtained geometrically.

**Fig. 2** Four PC plots describing the scatter of specimens across PC1 and PC2. Each PC plot represents a different epiphyseal aspect; A= Lateral aspect of the proximal epiphysis, B= Medial aspect of the proximal epiphysis, C= Anterior aspect of the distal epiphysis, D= Posterior aspect of the distal epiphysis. Specimens are grouped according to lineage. Transformation grids, at the extremes of each PC, show the relative deformation from the mean shape. Landmarks are linked by a wireframe in all transformation grids.

**Fig. 3** Transformation grids to demonstrate the relative change in shape from the smallest to the median and to the largest value of NLog centroid size for each epiphyseal aspect. Centroid sizes given in each grid are to 3 significant figures. Letters indicate epiphyseal aspect: A= Lateral aspect of the proximal

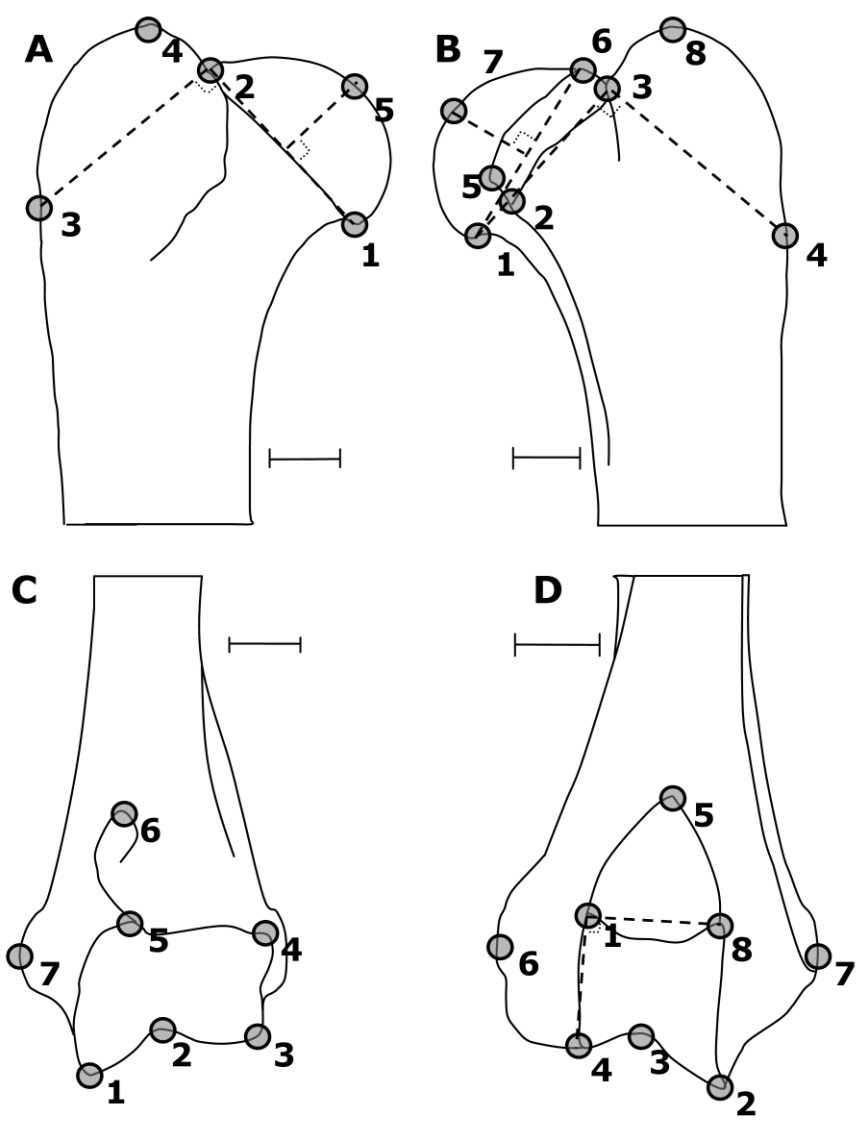
epiphysis, B= Medial aspect of the proximal epiphysis, C= Anterior aspect of the distal epiphysis, D= Posterior aspect of the distal epiphysis. The smallest NLog centroid size is exhibited by an individual of the species *Prionailurus planiceps* in all cases, excluding the anterior aspect of the distal epiphysis, where the smallest value is provided by a specimen of the species *Felis nigripes*.

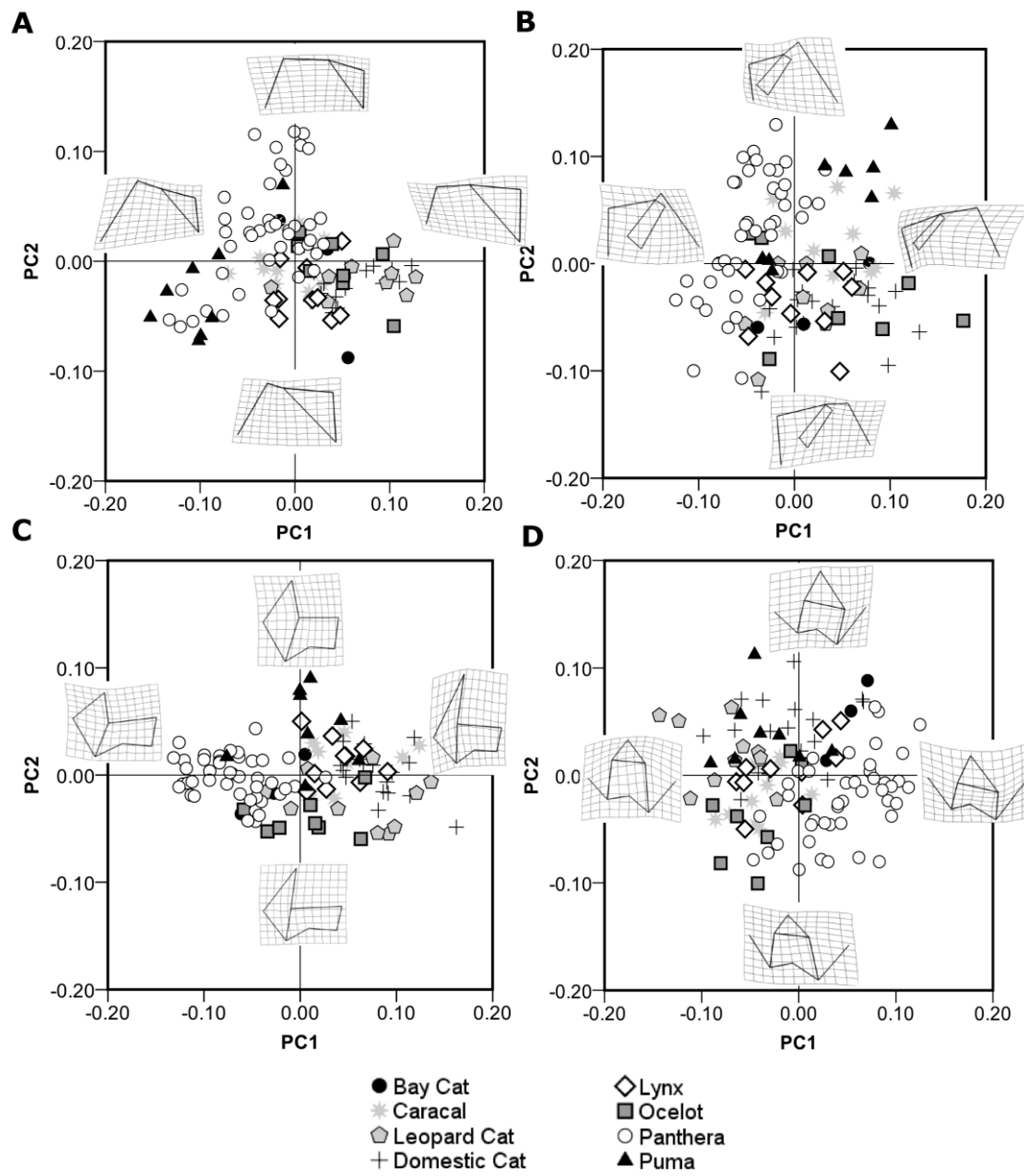
Specimens of *Caracal caracal* represent the median NLog centroid size in the case of the lateral and medial views of the proximal epiphysis. In the case of the distal epiphysis, specimens are of *Lynx lynx*. Finally, the largest NLog centroid size values are provided by specimens belonging to the species *Panthera leo* in the case of the proximal epiphysis. These values are provided by *Panthera tigris* specimens for the distal epiphysis.

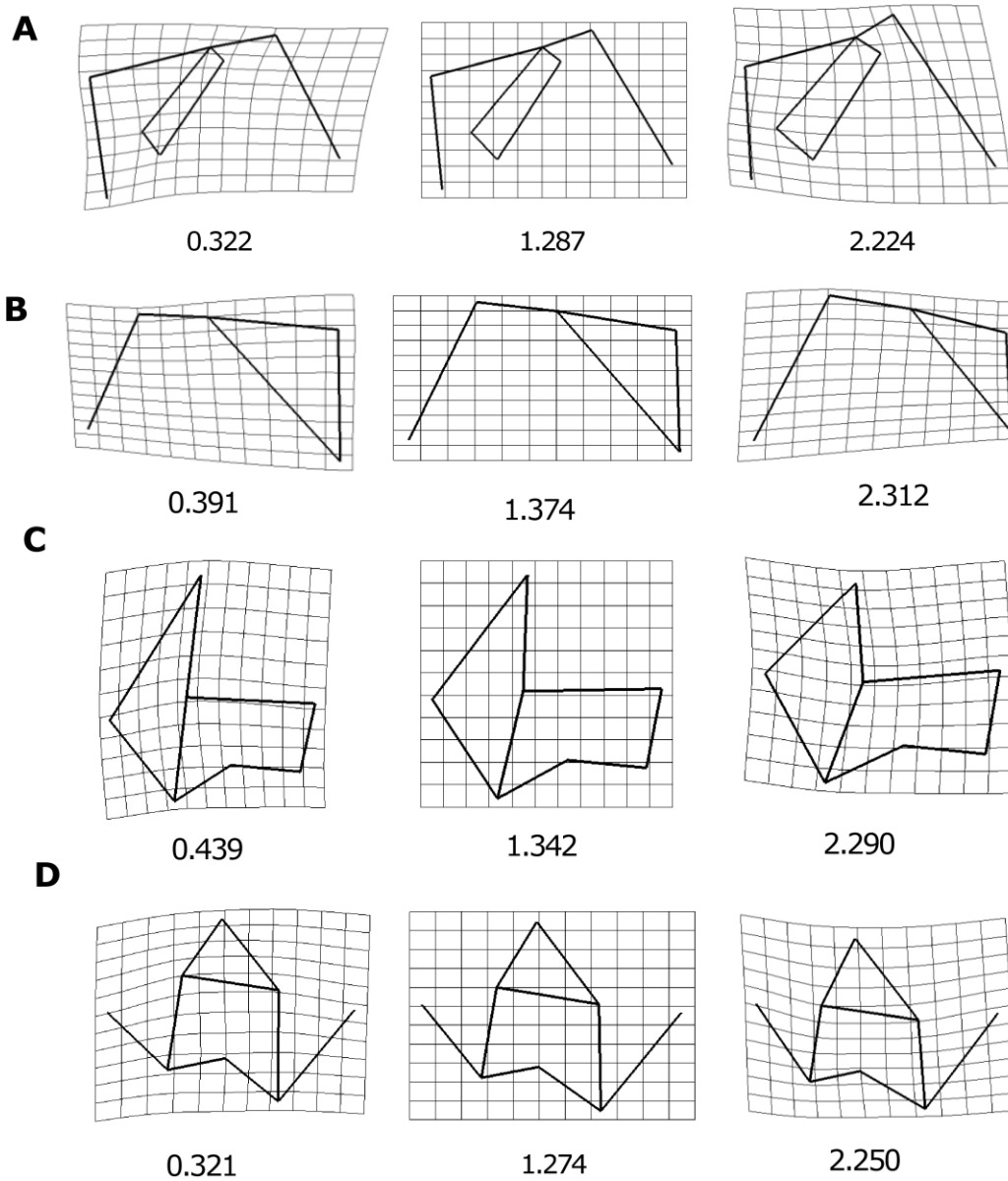
**Fig. 4** Four plots of function 1 vs. function 2 determined by DFAs. The scatter of specimens, categorised according to locomotor group, is shown, with group centroids included. Each plot represents a different epiphyseal aspect; A= Lateral aspect of the proximal epiphysis, B= Medial aspect of the proximal epiphysis, C= Anterior aspect of the distal epiphysis, D= Posterior aspect of the distal epiphysis. Transformation grids, at the extremes of each axis, show the relative deformation from the mean shape. Landmarks are linked by a wireframe in all transformation grids.

**Fig. 5.** Composite phylogeny of 32 extant species of Felidae showing character mapping based on squared-change parsimony (Maddison and Maddison, 2000)

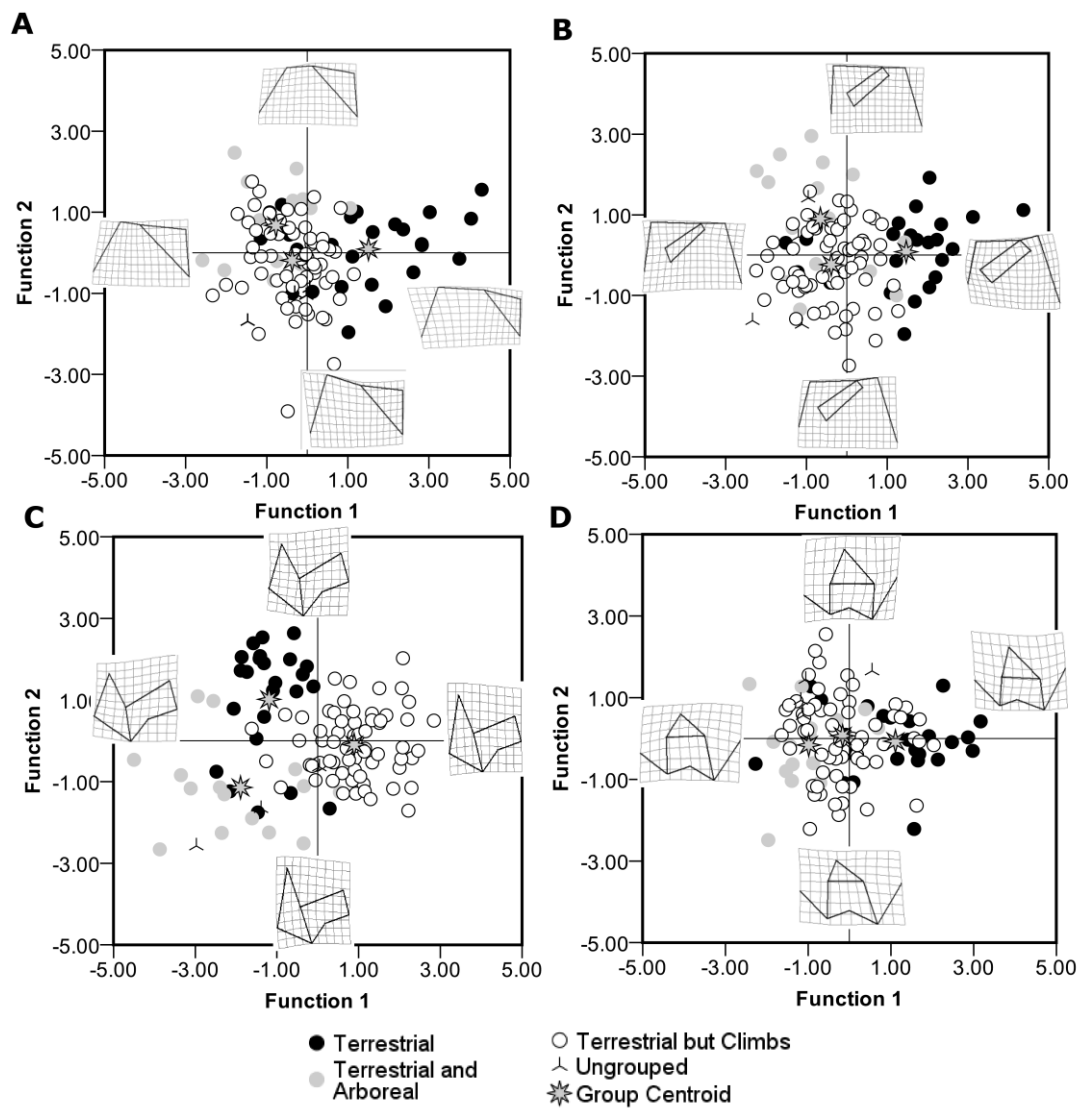
855 for PC1 species-averaged scores of the four epiphyses analysed. Time of  
856 divergence between species are expressed in millions of years.  
857 A= Lateral aspect of the proximal epiphysis, B= Medial aspect of the proximal  
858 epiphysis, C= Anterior aspect of the distal epiphysis, D= Posterior aspect of the  
859 distal epiphysis.

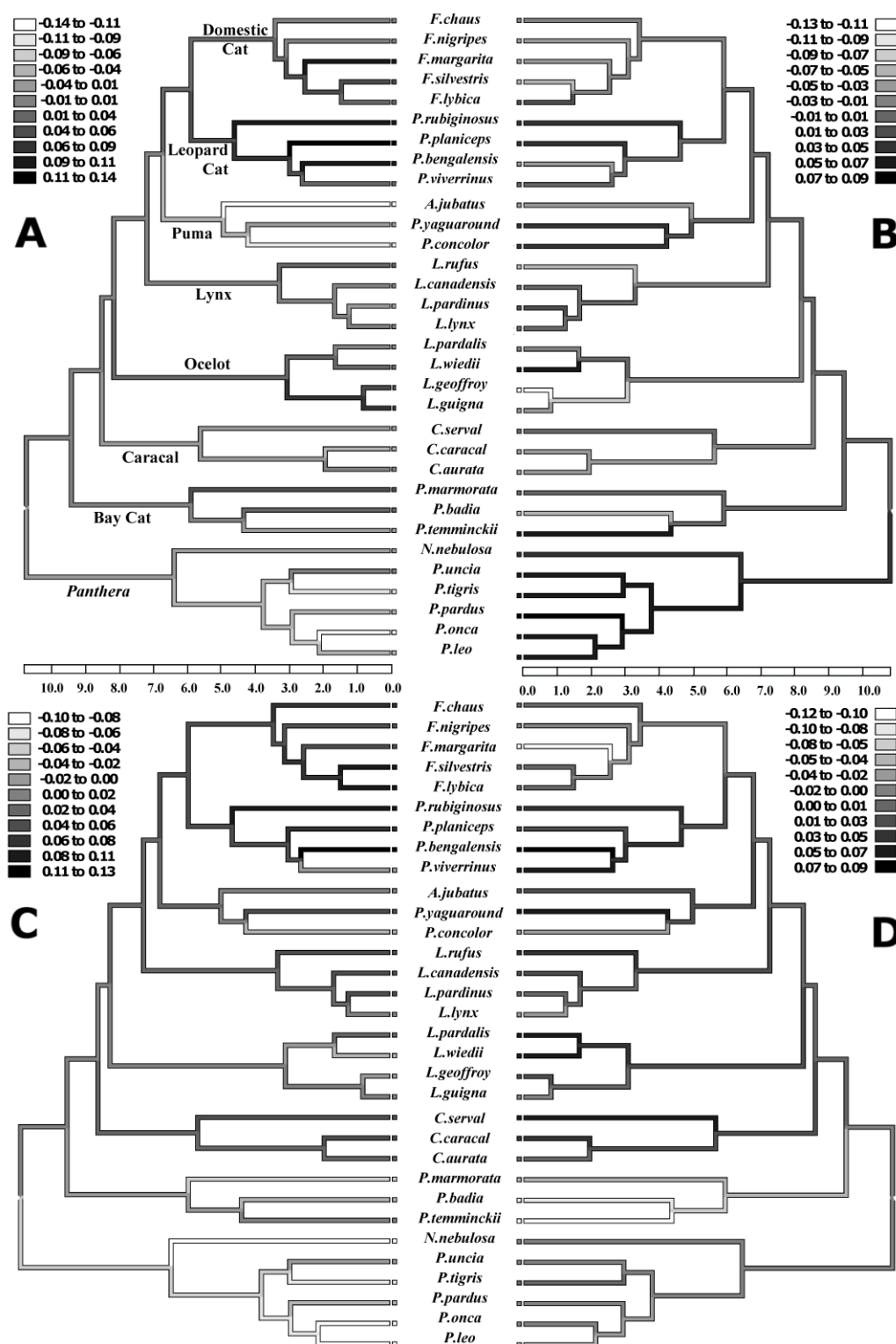












## TABLES

**Table 1** MANOVA statistic for each epiphyseal aspect, with phylogenetic categories as independent (X) and shape PCs as the dependent (Y) variables. The percentage of variance explained by phylogeny is displayed for each aspect. Significant P values are highlighted in bold.

<b>Epiphysis and aspect</b>	<b>Wilks' Lambda</b>	<b>F</b>	<b>Hypo d.f.</b>	<b>Error d.f.</b>	<b>% variance explained</b>	<b>P value</b>
Lateral aspect, proximal epiphysis	0.140	5.632	42	453.7	45.67	<b>&lt;0.0001</b>
Medial aspect, proximal epiphysis	0.032	5.050	84	559.2	33.97	<b>&lt;0.0001</b>
Anterior aspect, distal epiphysis	0.045	5.517	70	549.1	53.20	<b>&lt;0.0001</b>
Posterior aspect, distal epiphysis	0.028	5.326	84	565.3	35.67	<b>&lt;0.0001</b>

**Table 2** Statistic for multivariate regression testing allometry with Nlog size as independent (X) variable and shape PCs as dependent (Y). The percentage of variance explained by size is displayed for each epiphyseal aspect. Significant

<b>Epiphysis and aspect</b>	<b>Wilks' Lambda</b>	<b>F</b>	<b>Hypo d.f.</b>	<b>Error d.f.</b>	<b>% variance explained</b>	<b>P value</b>
Lateral aspect, proximal epiphysis	0.272	45.533	6	102	35.35	<b>&lt;0.0001</b>
Medial aspect, proximal epiphysis	0.207	30.568	12	96	20.07	<b>&lt;0.0001</b>
Anterior aspect, distal epiphysis	0.260	28.150	10	99	40.17	<b>&lt;0.0001</b>
Posterior aspect, distal epiphysis	0.205	31.394	12	97	17.01	<b>&lt;0.0001</b>

P values are highlighted in bold.

**Table 3** MANOVA statistic for each epiphyseal aspect with locomotion categories as independent (X) variables and all shape PCs as the dependent (Y). The percentage of variance explained by locomotion is displayed for each aspect. Significant P values are highlighted in bold. *Pardofelis temminckii*, *Pardofelis badia* and 2 of *Felis nigripes*, were excluded from MANOVA as the locomotor category of these individuals is unknown

Epiphysis and aspect	Wilks' Lambda	F	Hypo d.f.	Error d.f.	% variance explained	P value
Lateral aspect, proximal epiphysis	0.490	6.927	12	194	11.70	<b>&lt;0.0001</b>
Medial aspect, proximal epiphysis	0.449	3.731	24	182	4.83	<b>&lt;0.0001</b>
Anterior aspect, distal epiphysis	0.360	6.268	20	188	16.09	<b>&lt;0.0001</b>
Posterior aspect, distal epiphysis	0.494	3.239	24	184	8.96	<b>&lt;0.0001</b>

**Table 4** Wilks' Lambda values in addition to degrees of freedom and P values for both functions created in each DFA. Significant P values are highlighted in bold.

<b>Epiphysis and aspect</b>	<b>Function</b>	<b>Wilks' Lambda</b>	<b>d.f.</b>	<b>P value</b>
Lateral aspect,	DF1	0.535	6	<b>&lt;0.0001</b>
proximal epiphysis	DF2	0.916	2	<b>0.012</b>
Medial aspect,	DF1	0.518	10	<b>&lt;0.0001</b>
proximal epiphysis	DF2	0.864	4	<b>0.006</b>
Anterior aspect,	DF1	0.288	12	<b>&lt;0.0001</b>
distal epiphysis	DF2	0.690	5	<b>&lt;0.0001</b>
Posterior aspect,	DF1	0.682	6	<b>&lt;0.0001</b>
distal epiphysis	DF2	0.992	2	0.681

**Table 5** The composition of each function, showing the variables selected by stepwise procedure and the correlation coefficient (r) loaded on each function.

NLog\_CS = NLog centroid size, PC = Principal Component of shape variables.

<b>Epiphysis and aspect</b>	<b>Function 1</b>	<b>Function 2</b>
Lateral aspect, proximal epiphysis	PC2 0.793	PC3 0.819 PC6 0.561
Medial aspect, proximal epiphysis	PC7 0.589 NLog_CS 0.571 PC4 0.284	PC8 0.798 PC9 0.307
Anterior aspect, distal epiphysis	PC9 0.340	NLog_CS 0.731 PC1 -0.444 PC4 -0.439 PC8 0.321 PC3 0.285
Posterior aspect, distal epiphysis	NLog_CS 0.725	PC2 0.756 PC7 -0.650

**Table 6** Percentage of correctly classified cases after leave one out procedure, including an overall percentage for each epiphyseal aspect, and specific percentages for each locomotor group.

<b>Epiphysis and aspect</b>	<b>Total %</b>	<b>%Terrestrial</b>	<b>% Terrestrial and Arboreal</b>	<b>% Terrestrial but Climbs</b>
Lateral aspect, proximal epiphysis	62.9	75.0	60.0	59.1
Medial aspect, proximal epiphysis	64.8	83.3	60.0	59.1
Anterior aspect, distal epiphysis	83.0	79.2	62.5	89.4
Posterior aspect, distal epiphysis	50.0	66.7	62.5	40.9



**Table 7** Percentage of correctly reclassified specimens for each species in LAPE (lateral aspect of the proximal epiphysis), MAPE (medial aspect of the proximal epiphysis), AADE (anterior aspect of the distal epiphysis) and PADE (posterior aspect of the distal epiphysis). Predicted locomotor categories for the unknown specimens by each DFA are also listed in the table (T but CI = Terrestrial but Climbs; T and A = Terrestrial and Arboreal). # prox = Number of proximal specimens per species. # dist = Number of distal specimens per species

Species	# prox	# dist	LAPE	MAPE	AADE	PADE
<i>Acinonyx jubatus</i>	5	5	<b>100.00%</b>	<b>100.00%</b>	80.00%	40.00%
<i>Caracal aurata</i>	2	2	<b>100.00%</b>	0.00%	<b>100.00%</b>	50.00%
<i>Caracal caracal</i>	2	2	50.00%	50.00%	<b>100.00%</b>	<b>100.00%</b>
<i>Caracal serval</i>	6	6	50.00%	83.33%	<b>100.00%</b>	0.00%
<i>Felis silvestris lybica</i>	3	3	<b>100.00%</b>	33.33%	<b>100.00%</b>	33.33%
<i>Felis chaus</i>	2	2	<b>100.00%</b>	50.00%	<b>100.00%</b>	50.00%
<i>Felis margarita</i>	2	2	0.00%	0.00%	0.00%	0.00%
<i>Felis nigripes</i>	2	2	T but CI	T but CI	T but CI	T but CI
<i>Felis silvestris grampia</i>	9	9	44.44%	66.67%	<b>100.00%</b>	22.22%
<i>Leopardus geoffroy</i>	2	2	<b>100.00%</b>	50.00%	<b>100.00%</b>	50.00%
<i>Leopardus guigna</i>	1	1	0.00%	<b>100.00%</b>	<b>100.00%</b>	<b>100.00%</b>
<i>Leopardus pardalis</i>	4	4	75.00%	25.00%	75.00%	25.00%

<i>Leopardus wiedii</i>	1	1	0.00%	<b>100.00%</b>	<b>100.00%</b>	<b>100.00%</b>
<i>Lynx lynx</i>	3	3	33.33%	<b>100.00%</b>	<b>100.00%</b>	66.67%
<i>Lynx rufus</i>	1	1	<b>100.00%</b>	<b>100.00%</b>	<b>100.00%</b>	0.00%
<i>Lynx canadensis</i>	4	4	0.00%	0.00%	<b>100.00%</b>	50.00%
<i>Lynx pardinus</i>	2	2	<b>100.00%</b>	50.00%	50.00%	50.00%
<i>Neofelis nebulosa</i>	3	3	33.33%	33.33%	<b>100.00%</b>	<b>100.00%</b>
<i>Panthera leo</i>	17	17	<b>100.00%</b>	<b>100.00%</b>	<b>100.00%</b>	94.12%
<i>Panthera onca</i>	3	3	<b>100.00%</b>	0.00%	0.00%	0.00%
<i>Panthera pardus</i>	12	12	66.67%	50.00%	83.33%	58.33%
<i>Panthera tigris</i>	4	4	0.00%	50.00%	<b>100.00%</b>	25.00%
<i>Panthera uncia</i>	4	4	<b>100.00%</b>	<b>100.00%</b>	75.00%	50.00%
<i>Pardofelis badia</i>	1	1	T but CI	T and A	T and A	T and A
<i>Pardofelis marmorata</i>	1	1	<b>100.00%</b>	<b>100.00%</b>	<b>100.00%</b>	<b>100.00%</b>
<i>Pardofelis temminckii</i>	1	1	T but CI	T and A	T but CI	T and A
<i>Prionailurus bengalensis</i>	3	4	33.33%	<b>100.00%</b>	33.33%	66.67%
<i>Prionailurus planiceps</i>	1	1	0.00%	0.00%	0.00%	0.00%
<i>Prionailurus rubiginosus</i>	1	1	<b>100.00%</b>	<b>100.00%</b>	<b>100.00%</b>	<b>100.00%</b>
<i>Prionailurus viverrinus</i>	4	4	25.00%	75.00%	50.00%	0.00%
<i>Puma concolor</i>	2	2	0.00%	50.00%	50.00%	<b>100.00%</b>
<i>Puma jagouarundi</i>	1	1	0.00%	<b>100.00%</b>	<b>100.00%</b>	0.00%

---

**Table 8** Percentage of correctly classified cases after leave one out procedure with specimens of *Panthera leo*, *Felis silvestris* or *Neofelis nebulosa* individually excluded, including an overall percentage for each epiphyseal aspect, and specific percentages for each locomotor group. # Sample prox/dist = Number of specimens used in proximal epiphyseal analyses / Number of specimens used in distal epiphyseal analyses

	<b>Epiphysis and aspect</b>	<b>Total %</b>	<b>%Terrestria l</b>	<b>% Terrestrial and Arboreal</b>	<b>% Terrestrial but Climbs</b>
Excluding <i>P.leo</i> . # Sample prox/dist = 88/89	Lateral aspect, proximal epiphysis	54.5	71.4	53.3	53.0
	Medial aspect, proximal epiphysis	56.8	71.4	46.7	57.6
	Anterior aspect, distal epiphysis	83.1	85.7	56.3	89.4
	Posterior aspect, distal epiphysis	59.6	57.1	31.3	66.7
Excluding <i>F.silvestris</i> # Sample prox/dist = 96/97	Lateral aspect, proximal epiphysis	69.8	75.0	60.0	70.2
	Medial aspect, proximal epiphysis	62.5	70.8	60.0	59.6
	Anterior aspect, distal epiphysis	81.4	79.2	62.5	87.7
	Posterior aspect, distal epiphysis	58.8	66.7	56.3	56.1
Excluding <i>N.nebulosa</i> # Sample prox/dist = 102/103	Lateral aspect, proximal epiphysis	67.6	75.0	58.3	66.7
	Medial aspect, proximal epiphysis	69.6	75.0	66.7	68.2
	Anterior aspect, distal epiphysis	81.6	79.2	61.5	86.4
	Posterior aspect, distal epiphysis	64.1	66.7	61.5	63.6

**Table 9** Phylogenetic Generalised Least Squares models for locomotor categories or allometry, showing Wilks' Lambda, F test, degrees of freedom and probability values. Significant P values are highlighted in bold.

	<b>Epiphysis and aspect</b>	<b>Wilks' Lambda</b>	<b>F</b>	<b>d.f. 1</b>	<b>d.f. 2</b>	<b>P value</b>
<i>PGLS Locomotion</i>	Lateral aspect, proximal epiphysis	0.385	2.448	12.0	48.0	<b>0.0141</b>
	Medial aspect, proximal epiphysis	0.371	0.961	24.0	36.0	0.5317
	Anterior aspect, distal epiphysis	0.228	2.186	20.0	40.0	<b>0.0174</b>
	Posterior aspect, distal epiphysis	0.199	1.864	24.0	36.0	<b>0.0442</b>
<i>PGLS Size</i>	Lateral aspect, proximal epiphysis	0.403	6.169	6.0	25.0	<b>0.0005</b>
	Medial aspect, proximal epiphysis	0.234	5.179	12.0	19.0	<b>0.0008</b>
	Anterior aspect, distal epiphysis	0.494	2.147	10.0	21.0	0.0674
	Posterior aspect, distal epiphysis	0.191	6.708	12.0	19.0	<b>0.0001</b>